

# Creeping soil

Arjun M. Heimsath\* Department of Earth Sciences, Dartmouth College, Hanover, New Hampshire 03755, USA

John Chappell

Nigel A. Spooner

Danièle G. Questiaux

Research School of Earth Sciences, Australian National University, Canberra, ACT 0200, Australia

## ABSTRACT

Soil creep is the most widespread and perhaps the least understood process of erosion on soil-mantled hillslopes. Soil is slowly “stirred” by burrowing creatures, and particles are displaced in wetting-drying cycles. These actions can cause downslope creep by processes analogous to particle diffusion. Other possible transport mechanisms include shear and viscous-like creep, such that precise characterization of the entire process appears to require the tracing of labeled soil grains. Here we use natural quartz grains in a mature soil to determine grain movements from the time elapsed since each grain last visited the ground surface, measured by single-grain optical dating. Downslope flux is calculated from soil production by rock weathering at the soil base, measured with in situ-produced cosmogenic nuclide concentrations ( $^{10}\text{Be}$  and  $^{26}\text{Al}$ ). Results show that grains throughout the soil profile repeatedly visit the surface, and give the first quantitative characterization of grain-scale transport processes within creeping soil. These unique field data are interpreted with a Monte Carlo simulation to suggest that soil creep involves independent movements of mineral grains throughout the soil body and that grains are reburied or eroded by overland flow upon reaching the surface.

**Keywords:** erosion, optically stimulated luminescence, cosmogenic nuclides, southeastern Australia.

## SOIL CREEP

Hillslope soils typically are produced from weathering breakdown of the underlying bedrock (Carson and Kirkby, 1972; Dietrich et al., 1995; Heimsath et al., 1997). Setting aside landslides, which are likely to dominate soil erosion in steep terrain, soil moves slowly downhill by creep and slope wash. Observations from convex hills show that soil thickness decreases with increasing topographic curvature, supporting the view that creep occurs by diffusion-like processes with sediment flux linearly proportional to surface slope (Carson and Kirkby, 1972; Heimsath et al., 1999; Young, 1960). Such movement of individual soil grains could be caused by burrowing creatures (e.g., worms, ants, gophers) and by tree throw (trees uprooted, typically by high winds, often carry soil and bedrock attached to the root wad) coupled with localized slope wash, but field observations and laboratory studies show that nondiffusive processes may also occur, including shear and depth-dependent viscous-like flow (Carson and Kirkby, 1972; Fleming and Johnson, 1975; Selby, 1993; Young, 1960). Furthermore, observed relationships between soil depth and slope curvature on linear and compound slopes are incompatible with a simple linear relationship between sediment flux and surface slope alone (Braun et al., 2001; Heimsath et al., 2000; Roering et al., 1999).

Rods, blocks, and flexible tubes inserted in

the soil have been used to estimate creep processes (Fleming and Johnson, 1975; Young, 1960), but are too clumsy to examine grain-scale sediment transport, which requires the use of labeled particles (Selby, 1993). Insertion and detection of labeled grains throughout a soil mantle with microscale positional measurements would be a massive undertaking. Assuming, however, that grains brought to the surface by bioturbation and tree throw are buried again, vertical mixing at the grain scale may be determined by measuring the time since individual soil grains last visited the surface. We did this by single-grain optical dating, which is based on an optically stimulated luminescence (OSL) signal that accumulates within buried (below a few mm of the surface) quartz grains and is reset to zero by exposure to sunlight (Aitken, 1998; Huntley et al., 1985; Olley et al., 1999). Optical ages of grains from different depths depend on transport processes: e.g., grains moving in a surface layer would intermittently be exposed to sunlight, whereas grains never exposed at the surface should show “infinite” ages. Alternatively, mixing throughout the entire soil column would lead to finite-aged grains from soil surface to base.

Downhill movement of any soil grain resolves into slope-normal and slope-parallel components. Only the slope-normal velocity of a grain can be derived from its optical age. We cannot assess the slope-parallel velocity of individual grains, but the depth-averaged velocity can be calculated if the rate of soil pro-

duction from rock weathering is known at all points. Soil-production rates at our study site were previously determined from measurements of the in situ cosmogenic nuclides  $^{10}\text{Be}$  and  $^{26}\text{Al}$  (Heimsath et al., 2000) and are used in a new way here to derive slope-parallel velocities. In addition, modeling of the landscape evolution of the site (Braun et al., 2001) highlighted the need for more detailed field understanding of sediment transport processes active on soil-mantled landscapes.

## STUDY AREA

Our study landscape is a 1 ha granite-based hillslope draining to the Nunnock River in the upper Bega Valley in southeast New South Wales, Australia, used initially for the Heimsath et al. (2000) study. The site includes two spurs (convex noses) and an unchanneled hollow, and is morphologically similar to soil-mantled landscapes examined in northern California (e.g., Heimsath et al., 1997). Gradients range from 15% to 45%, and the entire surface is soil mantled, carrying an open *Eucalyptus* forest. Soil thickness ranges from 10 to 90 cm and increases with decreasing convex curvature. The top 10–15 cm is coarse sandy clay loam, and the main soil body is yellow-brown coarse sandy clay. The basal transition to the underlying granitic saprolite is sharp. Agents of soil mixing include the badger-sized Australian wombat, tree throw, worms, and burrowing ants, all of which show ability to penetrate the saprolite and incorporate it into the soil column. Microscope sections from undisturbed soil monoliths show evidence of repeated disruption throughout the column: fragmented ferriargillans; uncoated mineral grains in a structureless soil matrix; and absence of pedality.

Figure 1 (map) shows pit locations for soil depth (black filled circles) and radionuclide measurements (open circles), as well as for the OSL samples. We measured OSL on single grains from sets of quartz grains extracted from samples from near the top, middle, and bottom of each of the four numbered pits (except the shallow ridge-crest pit). Sample preparation followed standard OSL darkroom methods (Aitken, 1998), and OSL measurements followed a stepped regenerative procedure that determines the equivalent dose (ED) for each grain (Murray and Wintle, 2000; Olley et al., 1999). On the basis of OSL signals, grains divided into two groups: (1) those that

\*E-mail: Arjun.Heimsath@Dartmouth.edu.

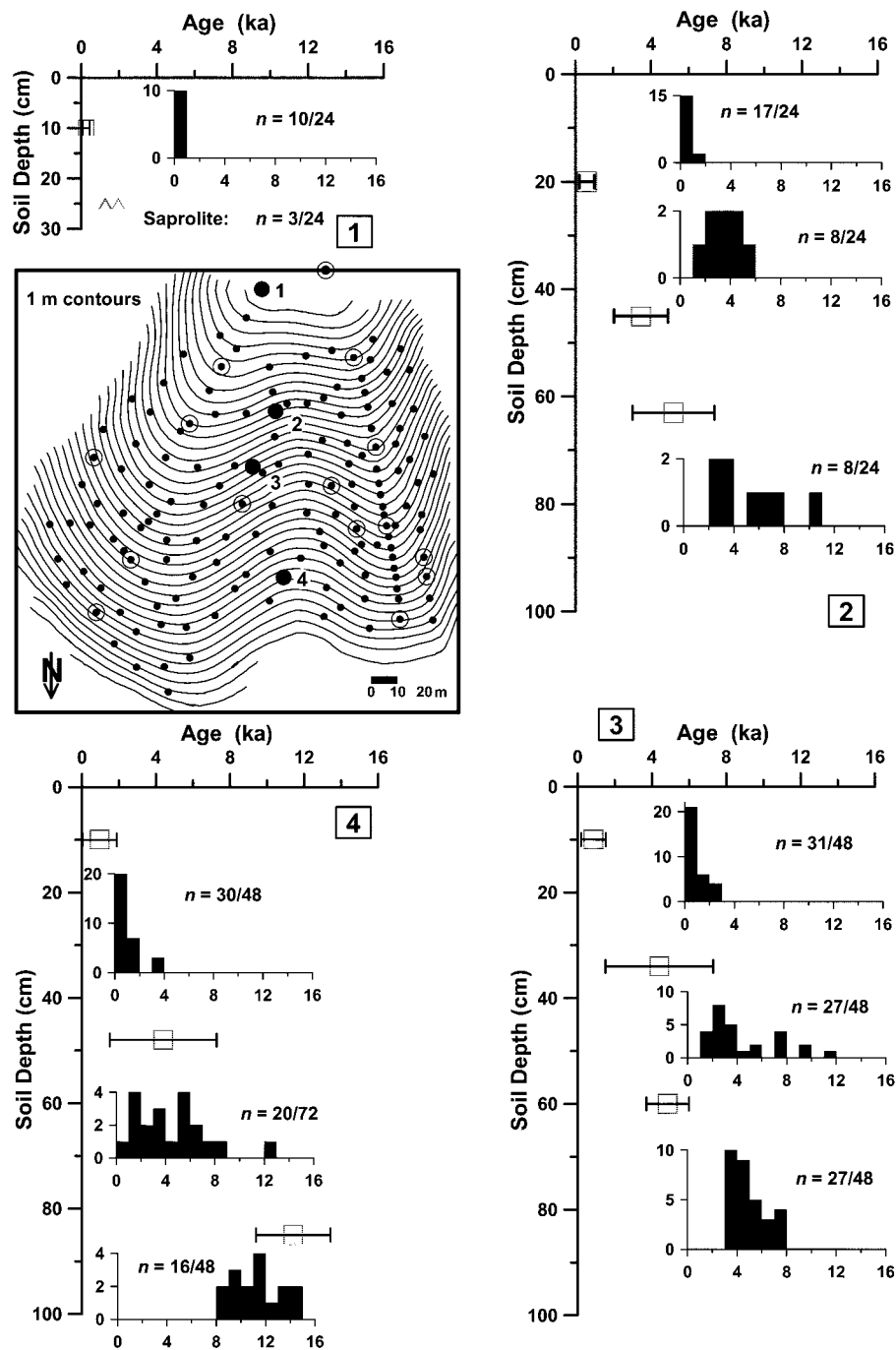


Figure 1. Histograms of single-grain optical dates from different depths in soil pits 1–4 (numbers in open squares; depths to saprolite are 18, 68, 65, and 90 cm, respectively); pit locations are numbered at large black circles on inset topographic site map (downslope is to north). Nuclide sample pits are shown by open circles; small black circles show pit locations used for morphometric analyses (Heimsath et al., 2000). At each histogram,  $n$  is proportion of finite-age grains in that sample. Open squares with error bars are variance-weighted means of grain ages (Table 1), plotted at appropriate sample depths. Saprolite at pit 1 recorded three bleached grains, indicating weak bioturbation effect, supported by field observations of saprolite penetration by roots and burrowing animals.

responded to applied  $\beta$  radiation and yielded finite OSL ages; and (2) those that showed no response to applied radiation. Measurements of the 375 C thermoluminescence (TL) peak, which significantly bleaches with <1 h exposure to daylight (Spooner et al., 1988), showed that all grains in the second group

were TL saturated (i.e., “infinite” TL age); tests with saprolite samples reliably identified infinite-age grains from the ratio of natural to laboratory-regenerated 375 C TL. For effectively infinite grains the luminescence has accumulated to the point that there are no empty traps in the crystal lattice left to fill (i.e., the

crystal has become saturated). For the local dose rates and quartz characteristics TL saturation is reached after 80–100 k.y. For finite-aged grains, the time since last exposure to sunlight (grain age) is ED divided by mean dose rate (DR) for each soil sample, which was determined from Th and K (neutron activation analysis) and from U (delayed neutron activation), together with in situ gamma scintillometry. DR was dominated by K in feldspar and clay, and variations throughout the soil are relatively small (average,  $3340 \pm 330 \mu\text{Gy/yr}$ ).

## RESULTS

Figure 1 shows histograms of grain ages and the proportions of surface-visiting (finite age) grains for each sample for each pit sampled for OSL measurements. Table 1 summarizes the OSL data and error-weighted mean ages and standard deviations. Several points emerge. (1) Samples from 10 cm depth have low mean ages (<1000 yr) and include grains with near-zero ages, but 35%–60% of the grains have not visited the surface. (2) Mean age increases with depth and exceeds 10 k.y. at the greatest depth (85 cm), but the proportion of surface-visiting grains is substantial even near the soil base. (3) Many grains must visit the surface several times, because mean ages of the finite-age grains are significantly less than the soil-residence time ( $t_{\text{res}}$ , Table 1) calculated by dividing soil depth by the soil-production rate, explained subsequently. (4) The fact that the ratio of age variance to age mean is large for most samples suggests that grain movements are independent and random.

Overall, results show that repeated grain displacements lead to mixing through the entire soil column as the soil moves downhill. Furthermore, the likelihood of displacement seems depth independent, because the net rates of grain movement downward from the soil surface are similar ( $V_{\text{vert}}$  in Table 1, calculated by dividing sample depth by its mean OSL age). Given that grain displacements are likely to have a downslope component, the results imply soil creep by diffusion-like movement of individual grains throughout the soil mass.

## MECHANISMS OF EROSION

To demonstrate the diffusion principle of sediment transport, we propose a conceptual model for individual grain displacement in the soil column. We numerically simulate downslope sediment movement with a Monte Carlo model in which grains are randomly displaced. Grains enter the model at soil base and describe a random walk through the soil body. Individual grains receive a series of independent random displacements of length  $\lambda$ , and the probability distribution,  $P(\lambda)$ , is assumed

TABLE 1. MEASUREMENTS AND RESULTS FROM OPTICAL DATES AND NUCLIDE-DETERMINED SOIL PRODUCTION RATES

	Depth (cm)	Cosmic ray dose rate (μGy/yr)	In situ water (%)	Sat. water (%)	U (ppm) (±5%)	Th (ppm) (±5%)	K (%) (±5%)	Total dose rate (μGy/yr)	ED (Gy)	Mean age (ka)	$V_{vert}$ (m/k.y.)	SlopeSoil flux (m <sup>2</sup> /k.y.)	Mean $V_{horiz}$ (m/k.y.)	
Pit 1	10	200 ± 30	9.7	30	1.17	7.12	2.58	3060 ± 230	0.87 ± 0.60	0.26 ± 0.18	0.26	2.3 50	2.1	12.0
	25	200 ± 30	8.2	29	2.16	7.32	2.37	3170 ± 230	<i>saprolite</i>	<i>saprolite</i>	n/a	n/a		
Pit 2	20	196 ± 30	9.1	31	1.98	7.88	2.86	3540 ± 270	2.00 ± 1.34	0.60 ± 0.40	0.19	5.6102	3.7	5.7
	45	190 ± 28	8.9	18	1.62	6.74	2.82	3350 ± 120	11.59 ± 4.78	3.47 ± 1.43	0.10	20.9		
Pit 3	63	187 ± 28	8.5	19	1.26	6.27	2.54	3020 ± 240	17.33 ± 7.25	5.19 ± 2.17	0.09	42.0		
	10	200 ± 30	13.7	31	2.56	9.13	3.09	3770 ± 170	2.84 ± 2.24	0.85 ± 0.67	0.14	2.3122	4.2	6.5
Pit 4	34	193 ± 29	8.4	32	1.69	5.64	2.32	2890 ± 140	14.70 ± 9.69	4.40 ± 2.90	0.09	12.6		
	60	187 ± 28	8.7	25	1.85	6.41	2.64	3230 ± 150	16.20 ± 3.84	4.85 ± 1.15	0.11	37.5		
Pit 4	10	200 ± 30	9.3	30	2.56	9.13	3.09	3940 ± 180	3.17 ± 3.11	0.95 ± 0.93	0.10	2.3170	5.0	5.9
	48	190 ± 28	11.8	17	1.85	6.41	2.64	3140 ± 150	14.66 ± 9.65	4.39 ± 2.89	0.13	23.6		
	85	180 ± 27	8.3	18	2.02	7.45	2.30	3060 ± 150	38.14 ± 6.71	11.42 ± 2.01	0.07	87.6		

Note: We used the improved single aliquot regenerative protocol (Murray and Wintle, 2000) and a type TL-DA-15 Risø TL/OSL reader providing 420–560 nm optical stimulation. UV emissions were detected from individual HF acid-etched 350–425 μm quartz grains. Illumination was for 125 s at 125 °C and the OSL signal was determined by subtracting the integral of the final 20 s from that of the first 20 s. Irradiations used a 40 mCi <sup>90</sup>Sr/<sup>90</sup>Y beta plaque delivering a dose rate of 0.097 ± 0.003 Gy/s. Dose-response curves were constructed using a 10 s preheat at 240 °C and five regenerative-dose steps ranging from 1.5 to 60 Gy, with a 3.0 Gy test dose. The α value was assumed to be 0.05 ± 0.02 (Thorne et al., 1999). Our dose-rate determination used updated conversion factors (Adamiec and Aitken, 1998) and the following beta particle attenuation factors: 0.76 ± 0.01 for U; 0.70 ± 0.01 for Th; 0.86 ± 0.01 for K.

to be symmetrical so that displacements upward from or down toward the soil base are equally probable. Model options for P(λ) are rectangular, triangular, and gaussian (in the latter two, the probability of a displacement occurring decreases with increasing λ), with a user-defined mean displacement length, λ. Displacements are assumed to be perpendicular to the soil surface and thus have a down-slope component λ tan(α), where α is slope angle. The user selects λ to be depth independent or to decrease with increasing soil depth. Grains that return to soil base remain stationary until the random generator gives them an upward displacement; grains that arrive at the surface have a user-defined probability, P<sub>w</sub>, of leaving the surface, which simulates loss to slope-wash, or “bounce” back into the soil body with probability (1 - P<sub>w</sub>). Soil depth is assumed to be in steady state, so that when a grain leaves, another enters at soil base; grains entering at soil base have an “in-

finite” age, and age is always reset to zero when a grain reaches the surface. By tracing individual grain histories, statistics for the ensemble of grain ages are determined at all depths (binned in 5 cm vertical intervals) for a series of downhill profiles 20 m apart (Fig. 2).

We explored a range of average step lengths (1–20 cm) and compared semigaussian and rectangular displacement probability distributions. Individual grains were followed for as many as 100 000 steps and each run traced 4000 grains. Statistics include the mean (N<sub>s</sub>) and standard deviation (S<sub>s</sub>) of the number of steps taken by grains at any point since their last surface exposure, as well as the percentage of grains that never visited the surface (V<sub>n</sub>). We multiply N<sub>s</sub> by a scaling factor, f, to determine the model age for each sample point using individual grain ages by OSL, A<sub>OSL</sub>,

$$f = \left( \sum A_{OSL} \right) / \left( \sum N_s \right). \quad (1)$$

Paired values in Table 2 compare results (upper value) for a typical model run with field observations from pits 2, 3, and 4 (pit 1 provides the upper boundary data); the comparisons are (1) mean model age versus mean OSL age, (2) N<sub>s</sub>/S<sub>s</sub> versus OSL mean age divided by standard deviation, and (3) V<sub>n</sub> (in percent) versus observed proportion of infinite-age grains. In this example, 20% of the grains leave the soil surface as slope wash, and mean displacement length is 5 cm at the soil surface and decreases to 1 cm at 80 cm depth. Each grain was traced for 20 000 displacements (equivalent to an average downhill travel distance of ~180 m at our site, where α is ~16°). Table 2 compares observations and model results for V<sub>n</sub> and for N<sub>s</sub>/S<sub>s</sub>, where model values of N<sub>s</sub> were rescaled with f = 0.85, calculated using equation 1 (this implies that the recurrence interval of model displace-

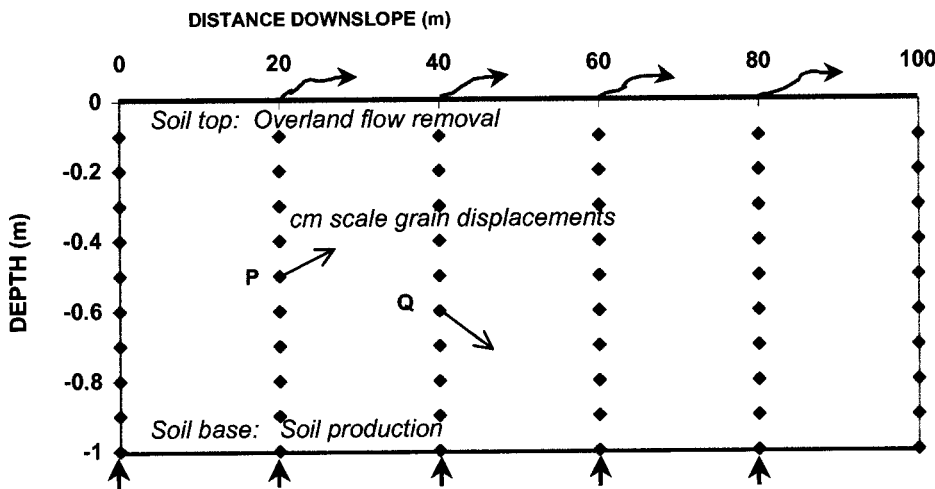


Figure 2. Monte Carlo model of soil-particle movement, shown horizontally for simplicity. Grains enter at upslope boundary and soil base (there is no evidence of eolian input or stratification in soil column) and can be removed from soil surface to simulate slope-wash losses. In soil column, particles move by centimeter-scale random displacements suggested by arrows from P and Q. Each downslope displacement has perpendicular component with equal probabilities of either upward or downward motion.

TABLE 2. MODEL VS. OPTICALLY STIMULATED LUMINESCENCE (OSL) RESULTS

Depth (m)	Age (k.y.)	N <sub>s</sub> /S <sub>s</sub>	V <sub>n</sub> (%)
Pit 2	0.2	1.3	40
	<i>0.6</i>	<i>1.5</i>	<i>29</i>
	0.45	4.3	53
	<i>3.5</i>	<i>2.4</i>	<i>67</i>
Pit 3	0.65	4.6	55
	<i>5.2</i>	<i>2.4</i>	<i>67</i>
	0.1	2.4	30
Pit 4	<i>0.9</i>	<i>1.3</i>	<i>35</i>
	0.35	3.9	45
	<i>4.4</i>	<i>1.5</i>	<i>44</i>
	0.6	4.6	55
	<i>4.9</i>	<i>4.2</i>	<i>44</i>
Pit 4	0.1	2.4	30
	<i>1</i>	<i>1</i>	<i>37</i>
	0.5	4.5	53
	<i>4.4</i>	<i>1.5</i>	<i>72</i>
	0.8	4.8	55
	<i>11.4</i>	<i>5.7</i>	<i>67</i>

Note: OSL data are in bold italics at each depth and the model age is N<sub>s</sub> times ε(H).

ments is equivalent to 0.85 yr). The agreement between model and observed data is quite good (the overall correlation coefficient for the Table is 0.64), but in this example the model overestimates mean ages at shallow depths and underestimates ages toward the soil base. Experiments found that different parameter settings can produce better agreement between model and observations for one variable (e.g., age), usually at the expense of agreement for another variable. Overall, the model simulates the observations reasonably well, and we infer that sediment transport at the study site is dominated by mixing of grains throughout the soil profile in conjunction with an en masse creeping of the soil, and that a significant proportion of the grains that reach the surface is transported from the slope by surface wash.

The mean downslope velocity of soil creep indicated by the model is the depth-averaged value of  $\Lambda/f$  cm/yr. For the run represented in Table 2, this gives  $\sim 3.5$  cm/yr. This result can be compared with slope-parallel velocity derived from soil-production rates, which have been determined from cosmogenic nuclide measurements at our study area (Heimsath et al., 2000). Cosmogenic nuclide concentrations in bedrock have been widely used to infer erosion rates, and the methodology was adapted to determine soil-production rates (Heimsath et al., 1997). Specifically, cosmogenic  $^{10}\text{Be}$  and  $^{26}\text{Al}$  concentrations directly beneath the soil base at a range of soil pits showed that the soil-production rate,  $\epsilon$ , decreases with increasing soil thickness,  $H$ ,

$$\epsilon(H) = \epsilon_0 e^{(-\alpha H)}, \quad (2)$$

where  $\epsilon_0 = 53 \pm 3$  m/m.y. and  $\alpha = 2.0 \pm 0.1$  1/m at the study site. Soil depth is known in detail (Heimsath et al., 2000), allowing us to integrate equation 2 along a downslope flow line passing near the sample pits to obtain soil flux. Dividing flux by local soil depth gave depth-averaged downslope velocity near each pit (mean  $V_{\text{horiz}}$  in Table 1).

## DISCUSSION AND CONCLUSIONS

Depth-averaged velocities derived from soil production are similar for pits 2–4; the average is 6.0 m/k.y., substantially less than the Monte Carlo model run shown in Table 2, which was 35 m/k.y. Several factors can cause the Monte Carlo results to be too high. First, the model assumes no cohesion in the soil, which is unlikely (Selby, 1993). Second, the

larger the mean displacement,  $\Lambda$ , the slower the downslope velocity given by the model, because scaled frequency of displacements decreases approximately as  $\Lambda^2$ . It seems likely that displacements at our field site are larger and less frequent than the value of a few centimeters every year used for Table 2, given that the principal agents of disturbance are burrowing wombats and tree throw. This is consistent with our OSL age data from near soil base, which show less variance than predicted by the Monte Carlo model (high values of  $N_s/S_s$ ) and imply that aggregates of grains visited the surface and were reburied at about the same time, presumably because of an isolated large disturbance.

A significant fraction of total mass wasting may be mineral solution from below the soil base, in which case our estimates of  $V_{\text{horiz}}$  (Table 1) would be too large because net soil production would be less than that given by equation 2. Mass loss by solution is not detected from in situ cosmogenic nuclide concentrations from below the soil base, which determine the overall lowering rate by mechanical weathering, subject to the steady-state assumption (Heimsath et al., 1997, 2000). Measurements from soil-covered granitic slopes elsewhere (Selby, 1993; Stonestrom et al., 1998) show solution losses equivalent to lowering rates of  $\sim 2$ – $14$  m/m.y. If similar conditions apply, solution could contribute significantly to lowering at our study site, because the average lowering rate given by equation 2 for our downhill transect is  $\sim 20$  m/m.y., but the effect of solution has yet to be evaluated in the study area. Solution, however, will not affect downhill grain diffusion throughout the depth of the soil, which our results show to be the major if not dominant process in soil creep.

## ACKNOWLEDGMENTS

We thank Dave Furbish for significant improvement in our modeling efforts, Jon Olley for valuable discussion, and the site landowner, Steve Bateman, for site access. Damien Kelleher helped survey the site, N. Hill helped with sample preparation, and B. Minty analyzed the in situ gamma scintillometry. The U.S. National Science Foundation partly supported this work (grant to Heimsath). D. Furbish and an anonymous reviewer provided very helpful comments.

## REFERENCES CITED

Adamiec, G., and Aitken, M.J., 1998, Dose-rate conversion factors: Update: *Ancient TL*, v. 16, p. 37–50.  
 Aitken, M.J., 1998, *An introduction to optical dating*: Oxford, Oxford University Press, 267 p.

Braun, J., Heimsath, A.M., and Chappell, J., 2001, Sediment transport mechanisms on soil-mantled hillslopes: *Geology*, v. 29, p. 683–686.  
 Carson, M.A., and Kirkby, M.J., 1972, *Hillslope form and process*: New York, Cambridge University Press, 475 p.  
 Dietrich, W.E., Reiss, R., Hsu, M.-L., and Montgomery, D.R., 1995, A process-based model for colluvial soil depth and shallow landsliding using digital elevation data: *Hydrological Processes*, v. 9, p. 383–400.  
 Fleming, R.W., and Johnson, A.M., 1975, Rates of seasonal creep of silty clay soil: *Quaternary Journal of Engineering Geology*, v. 8, p. 1–29.  
 Heimsath, A.M., Dietrich, W.E., Nishiizumi, K., and Finkel, R.C., 1997, The soil production function and landscape equilibrium: *Nature*, v. 388, p. 358–361.  
 Heimsath, A.M., Dietrich, W.E., Nishiizumi, K., and Finkel, R.C., 1999, Cosmogenic nuclides, topography, and the spatial variation of soil depth: *Geomorphology*, v. 27, p. 151–172.  
 Heimsath, A.M., Chappell, J., Dietrich, W.E., Nishiizumi, K., and Finkel, R.C., 2000, Soil production on a retreating escarpment in south-eastern Australia: *Geology*, v. 28, p. 787–790.  
 Huntley, D.J., Godfrey-Smith, D.I., and Thewalt, M.L.W., 1985, Optical dating of sediments: *Nature*, v. 313, p. 105–107.  
 Murray, A.S., and Wintle, A.G., 2000, Luminescence dating of quartz using an improved single-aliquot regenerative-dose protocol: *Radiation Measurements*, v. 32, p. 57–73.  
 Olley, J.M., Caitcheon, G.G., and Roberts, R.G., 1999, The origin of dose distributions in fluvial sediments, and the prospect of dating single grains from fluvial deposits using optically stimulated luminescence: *Radiation Measurements*, v. 30, p. 207–217.  
 Roering, J.J., Kirchner, J.W., and Dietrich, W.E., 1999, Evidence for non-linear, diffusive sediment transport on hillslopes and implications for landscape morphology: *Water Resources Research*, v. 35, p. 853–870.  
 Selby, M.J., 1993, *Hillslope materials and processes*: Oxford, Oxford University Press, 451 p.  
 Spooner, N.A., Prescott, J.R., and Hutton, J.T., 1988, The effect of illumination wavelength on the bleaching of the thermoluminescence (TL) of quartz: *Quaternary Science Reviews*, v. 7, p. 325–329.  
 Stonestrom, D.A., White, A.F., and Akstin, K.C., 1998, Determining rates of chemical weathering in soils—Solute transport versus profile evolution: *Journal of Hydrology*, v. 209, p. 331–345.  
 Thorne, A., Grün, R., Mortimer, G., Spooner, N.A., Simpson, J.J., McCulloch, M., Taylor, L., and Curroe, D., 1999, Australia's oldest human remains: Age of the Lake Mungo 3 skeleton: *Journal of Human Evolution*, v. 36, p. 591–612.  
 Young, A., 1960, Soil movement by denudational processes on slopes: *Nature*, v. 188, p. 120–122.

Manuscript received July 5, 2001

Revised manuscript received October 17, 2001

Manuscript accepted October 22, 2001

Printed in USA